

# Binary Neural Networks for Memory-Efficient and Effective Visual Place Recognition in Changing Environments

Bruno Ferrarini<sup>1</sup>, Michael Milford<sup>2</sup>, Klaus D. McDonald-Maier<sup>1</sup> and Shoaib Ehsan<sup>1</sup>

**Abstract**—Visual place recognition (VPR) is a robot’s ability to determine whether a place was visited before using visual data. While conventional hand-crafted methods for VPR fail under extreme environmental appearance changes, those based on convolutional neural networks (CNNs) achieve state-of-the-art performance but result in model sizes that demand a large amount of memory. Hence, CNN-based approaches are unsuitable for memory-constrained platforms, such as small robots and drones. In this paper, we take a multi-step approach of decreasing the precision of model parameters, combining it with network depth reduction and fewer neurons in the classifier stage to propose a new class of highly compact models that drastically reduce the memory requirements while maintaining state-of-the-art VPR performance, and can be tuned to various platforms and application scenarios. To the best of our knowledge, this is the first attempt to propose binary neural networks for solving the visual place recognition problem effectively under changing conditions and with significantly reduced memory requirements. Our best-performing binary neural network with a minimum number of layers, dubbed FloppyNet, achieves comparable VPR performance when considered against its full precision and deeper counterparts while consuming 99% less memory.

## I. INTRODUCTION

Visual place recognition addresses the problem of determining whether a location has been visited before using visual information. VPR is a fundamental task for autonomous navigation as it enables a robot to re-localize itself in the work space when the position tracking fails or drifts due to accumulated errors. However, variations in viewpoint and appearance due to seasonal, weather and illumination changes render VPR a challenging problem for mobile robots. While conventional hand-crafted techniques for VPR fail under extreme environmental changes, those based on deep CNNs achieve state-of-the-art performance [46] but result in model sizes that demand a large amount of memory.

Mobile robots are often equipped with resource-constrained hardware that limits the usability of such demanding techniques [34], [15]. Saving memory without sacrificing the performance is paramount for such resource-constrained mobile robots. Indeed, a small-sized model would enable VPR on cheap hardware and would allow allocation of extra resources

This work was supported by the UK Engineering and Physical Sciences Research Council through grants EP/R02572X/1, EP/P017487/1, and in part by the RICE project funded by the National Centre for Nuclear Robotics Flexible Partnership Fund.

<sup>1</sup>Bruno Ferrarini, Klaus D. McDonald-Maier and Shoaib Ehsan are with the School of Computer Science and Electronic Engineering, University of Essex, Colchester, CO4 3SQ, UK {bferra, kdm, sehsan}@essex.ac.uk

<sup>2</sup>Michael Milford is with the QUT Centre for Robotics, School of Electrical Engineering and Robotics and the Australian Centre for Robotic Vision at the Queensland University of Technology, and was partially supported by ARC grants FT140101229, CE140100016 and the QUT Centre for Robotics. michael.milford@qut.edu.au

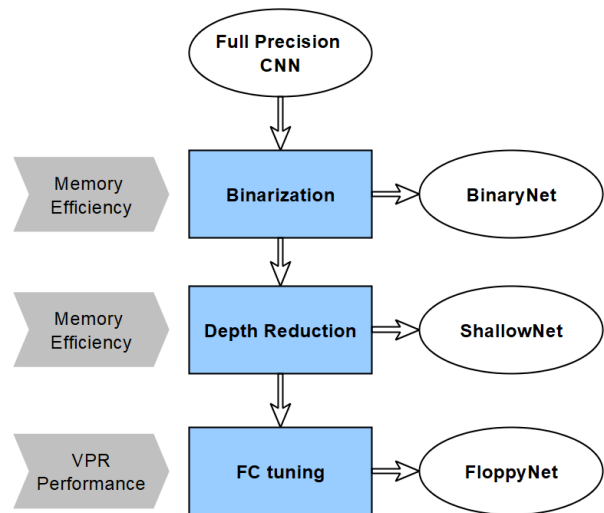


Fig. 1. The proposed approach consists of three steps: Binarization reduces the model size by about 97%. Depth reduction decreases the number of layers for further model size reduction. The subsequent performance loss due to binarization is mostly countered by training the network with a properly tuned fully connected stage including full precision neurons.

for additional functionalities to improve a robot’s navigation system. Reducing memory demand while keeping VPR performance at a reasonable level is a difficult task. To tackle this challenge, in this paper we propose the multi-step approach shown in Figure 1 that combines Binary Neural Networks (BNNs) [12], [23] and depth reduction to obtain very compact models that drastically decrease the memory requirements. The subsequent VPR performance loss is mostly countered by training the model with a classifier stage including a reduced number of full precision neurons.

Binary neural networks are a class of CNNs characterized by a single bit precision for both weights and activations instead of the 32 bits used by conventional deep networks. So far, BNNs have been employed and highly optimized for classification tasks only, where they exhibit lower yet comparable accuracy to their full precision counterparts [40], [4]. However, classification and VPR are different problems. The first aims to find the best fit among categories, while VPR consists of matching different images of the same scene. To the best of our knowledge, this paper is the first attempt to employ BNNs to solve the VPR problem effectively under environmental changes and with significantly reduced memory requirements. Our best model<sup>1</sup>, dubbed FloppyNet, achieves comparable VPR performance to its full precision and deeper counterparts while consuming 99% less memory. With a model

<sup>1</sup>Authors will share the model and source code upon the publication.

size of 154 Kilobytes, FloppyNet can therefore be stored on an old single-sided 5<sup>1/4</sup> floppy disk!

The rest of this paper is organized as follows. Section II presents an overview of the related work. Section III presents our multi-step approach to obtain compact BNNs for VPR. The evaluation criteria and the experimental setup are described in Section IV. Results are presented and discussed in Section V. Conclusions are drawn in Section VI.

## II. RELATED WORK

### A. Visual Place Recognition

Environmental changes, such as illumination and viewpoint variations, render VPR a very challenging task. As the core problem of VPR is image matching, computing a robust image representation is fundamental for developing reliable localization systems in dynamic environments. In recent years, machine learning techniques have become more and more popular in VPR applications. CNN-based methods achieve high performance in various environmental conditions [48] and under viewpoint variations [47]. A pre-trained CNN for a different task can be used off-the-shelf for generating an image descriptor in place of handcrafted local and global image descriptors, such as SIFT [32] and Histogram-of-Oriented Gradients (HOG) [17], [13]. For example, the features computed by the convolutional layers of AlexNet [29] can be used to match place images. How *et al.* [21] showed that the features extracted from *conv3* layer of AlexNet are robust to condition variations, while those from *pool5* work well for viewpoint changes. Bai *et al.* [6] used those layers' features to improve the matching performance of SeqSLAM [36] under viewpoint changes. AMOSNet and HybridNet [8] are variants of AlexNet trained on Specific PlaceEs Dataset (SPED) [8] in order to compute more specific image representations for VPR. PlaceNet [49] is based on the same idea, but it uses VGG-16 [41], which is trained on a large dataset, dubbed Places365, organized in 365 place categories. Cross-Region-Bow [9], the regional maximum activation of convolutions (R-MAC) [45], CAMAL [27] and Region-VLAD [26], focus on features pooling from a pre-trained network as they consider feature extraction and aggregation as two separated stages. On the other hand, NetVLAD [5] consists of two stages that are trained end-to-end. The first is a VGG-16 network that extracts the features from an image followed by an aggregation layer to combine them in a VLAD-like descriptor [25].

### B. Binary Neural Networks

While CNNs are effective in addressing VPR, they include many parameters that result in large model sizes. In the last decade or so, several techniques have been proposed to decrease models' memory requirements. Early approaches targeted redundant and non-informative weights: Optimal Brain Damage [30] and Optimal Brain Surgeon [20] decrease the number of connections using the Hessian of the loss function. Han *et al.*, [19] showed how to reduce the number of parameters by one order of magnitude in several state-of-the-art networks by weight pruning. Also, a model's size can be

shrunk by lowering the precision of the weight. However, post-quantization yields performance loss, which is more prominent as the precision lowers. In particular, binarization (1-bit precision) impacts heavily on a classifier's accuracy [11].

Binary-aware training allows low precision models with acceptable classification accuracy [40]. Although training binary models from scratch was attempted decades ago [38], only recently, gradient-based techniques have become applicable to BNNs. Courbariaux *et al.* [12] trained a full binary network for the first time using Straight-Through-Estimator (STE) [7]. The key idea of STE is to keep in memory real-valued weights, which are binarized only in the forward pass to compute neurons' activation and updated during back-propagation as in a standard neural network. Afterwards, several additions to the field were proposed to improve BNNs. In XNOR-Net [37], the convolutional blocks are rearranged to increase classification accuracy. Batch-Normalisation (BatchNorm) is usually placed after the convolution and before the activation function. In XNOR-Net, BatchNorm and binary activation precede convolution so that pooling occurs before binarization. DoReFa-Net [50] exploits bit-wise operations to compute the dot product between a layer's weights and the inputs in an efficient way to speed-up training. In [14], binarization threshold is learned along with the weights to shorten the accuracy gap with full precision classifiers. Networks using less extreme quantization have been proposed as a more accurate alternative to binary networks. Ternary networks [31], [51] use three values to encode weights. Although they exhibit a significant memory reduction and simple arithmetic, ternary networks require 2-bits to store weights and do not outperform BNNs by a wide margin [40].

To the best of our knowledge, BNNs have been used only for classification so far. Unlike regular CNNs, BNNs have not been considered for VPR yet. This paper aims to contribute to the field by proposing a highly compact class of binary networks to solve the VPR problem effectively in changing environments.

## III. BINARY NEURAL NETWORKS FOR VPR

This section presents a new class of binary neural networks for visual place recognition and provides implementation details. To achieve memory efficiency while maintaining reasonable VPR performance, we propose a multi-step approach to turn a standard CNN into a compact yet effective feature extractor. These steps are: binarization, depth reduction, and tuning of the fully connected stage.

### A. Binarization

Binarization addresses memory efficiency. The use of 1-bit precision for the weights decreases a model's size dramatically by about 97%. Storing a 32-bit weight requires four bytes while a single bit is needed for a binary one. Hence, a binary model can be up to 32 times smaller than its full precision counterpart. Training a binary model with a reasonable performance gap from its full precision counterpart requires applying specific techniques and some network structure adjustments. This section has the two-fold purpose of describing

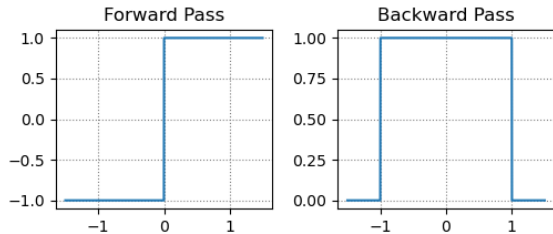


Fig. 2. Sign quantizer in forward and backward passes.

the implementation criteria we have taken and giving a gentle introduction to Binary Neural Networks.

1) *Training and Binary Function*: Training BNNs with backpropagation is not applicable as it requires sufficient precision to allow gradient accumulation to work [23]. Courbariaux *et al.* solved this problem [12] with Straight Through Estimator (STE) [7]. The fundamental idea of STE is that the quantization function is applied in the forward pass but skipped during backpropagation. STE keeps a set of full precision weights denoted as proxies ( $W_F$ ) which are binarized ( $W_B$ ) within the network on forward pass to make a prediction and compute a loss. Any function can be used as binarization function. Courbariaux *et al.* use *sig* function:

$$W_B = \text{sig}(W_F) \quad (1)$$

In the backpropagation phase,  $W_F$  are updated accordingly to the loss gradient as in a regular network:

$$\frac{\partial L_{\text{loss}}}{\partial W_F} = \frac{\partial L_{\text{loss}}}{\partial W_B} \quad (2)$$

Activations are binarized in the forward pass similarly to the weights. Courbariaux *et al.* observed that canceling the gradient when activation exceeds 1.0 improves a model's accuracy.

$$\frac{\partial L_{\text{loss}}}{\partial a_F} = \begin{cases} \frac{\partial L_{\text{loss}}}{\partial W_B}, & \text{if } |a_F| \leq 1 \\ 0, & \text{otherwise} \end{cases} \quad (3)$$

Figure 2 shows the plots for *sig* quantizer in the forward and backward passes.

The binary models presented in this work use *sig* as a quantizer and are trained with Larq [18]. Larq is a framework built on top of Keras [10] which offers full support to train BNNs with STE.

2) *Encoding Values*: Binary encoding of weights and activations reduces dot products to a series of bit-wise operations. In particular, representing logical '0' and '1' with  $-1$  and  $1$  renders convolutions and matrix multiplications a series of XNOR and pop-count operations [12]. However, to exploit the efficiency of binary operations, a dedicated GPU kernel or specific hardware is required [12], [23]. A conventional computation engine stores binary weights into 32-bit variables. As a result, multiply-accumulate operations (MAC) in BNN require the same time and resources as in a full precision network. A dedicated GPU kernel would concatenate 32 binary variables into a 32-bit register and evaluate them altogether

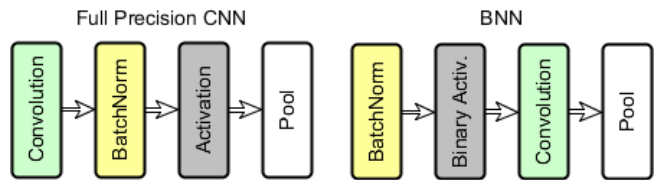


Fig. 3. Convolution blocks in a CNN (left) and in a BNN (right).

using bitwise operations. Binary MACs can be implemented as follows:

$$a_1 += \text{popcount}(\text{xnor}(a_o^{32}, w_1^{32})) \quad (4)$$

where  $a_o^{32}$  and  $w_1^{32}$  are sets of 32 inputs and weight. For example, a Compute Capability 8.0 NVIDIA GPU [1] computes XNOR and bitwise sum in 1 clock cycle and popcount in 4 cycles. This results in  $32/6 = 5.3$  MACs per clock cycle. [23].

This paper focuses on VPR performance. The implementation of a binary-aware GPU kernel is out of scope for this particular work. The expected computational efficiency for the proposed models is estimated from the network structure and binary parameter number.

3) *Batch Normalization*: Batch Normalisation (BatchNorm) [24] uses mini-batch statistics during training to adjust and scale activations. The central role of BatchNorm in full precision networks is to speed up the training. In BNN, BatchNorm is essential as it improves performance and helps training convergence [4], [39], [40]. It is worth mentioning that the parameters of BatchNorm layers cannot be binarized; however, they are few compared with the number of weights and do not contribute significantly to the model size. (Table II).

4) *Layers Order*: A convolution block in a CNN consists of convolution, BatchNorm, Activation and Pool. BNNs achieve better performance if the order of the layers is as follows: BatchNorm, Binary Activation, Binary convolution and Pool [37]. This layer arrangement has a two-fold purpose. First, it allows for pooling from real values before binarization. Otherwise, the result would be a tensor dense in 'ones' which is proven to affect the accuracy of a BNN negatively [4]. Second, BatchNorm can replace bias as it works as a threshold for the subsequent layer [39], [40]. As bias parameters cannot be binarized, not using them reduces the memory and the number of 32-bit MACs in binary networks. The BNNs implemented for this work do not use bias but use BatchNorm modules instead.

In the rest of this paper, the term convolution block implies the presence of BatchNorm in the proper position as shown in Figure 3.

5) *First Layer input*: Full precision inputs are recommended to improve a model's precision [23] and do not increase the model size since the weights are binary. Accordingly with this consideration, the binary networks presented in this work have the first convolution layer directly connected to the input image with no binary activation and BatchNorm placed in the middle.

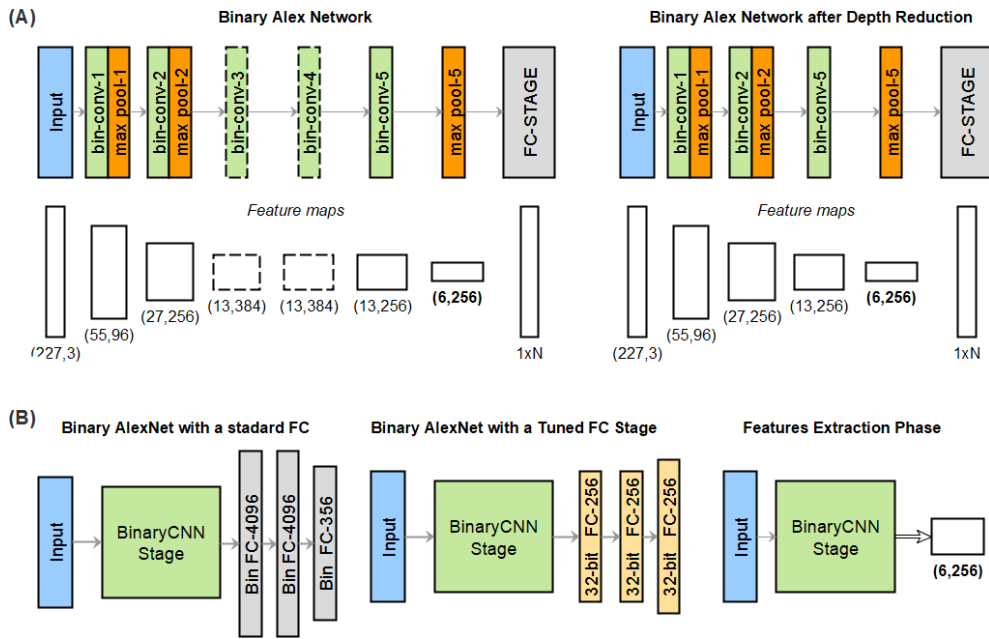


Fig. 4. Depth Reduction (A) and FC tuning (B) applied to AlexNet structure. In this example, depth reduction consists of removing conv3 and conv4 layers. The three pooling layers are kept to maintain the same shape of the output feature map at pool5.

### B. Depth Reduction

The primary motivation for depth reduction is to save even more memory. Networks for classification are deep and can have dozens of convolution levels [28]. However, VPR is a different task and we empirically found that it is possible to achieve good performance with fewer layers and weights. Not only the model size but also the computational efficiency of the network benefits from depth reduction. For example, our best model is obtained by removing the two intermediate convolution layers from an AlexNet-like CNN as shown in Figure 4.A. This operation decreases by 66% the convolution weights amount yielding both model size and MACs reduction.

### C. Tuning of the Fully Connected Stage

BNNs are highly optimized for the classification. The fully connected (FC) stage of classifiers is often populated with a large number of neurons. AlexNet and VGG16, for example, include 4096 units in each layer. When it comes to training a model for VPR, the hyper-parameters of the FC layers should be revised. Our best binary model is trained using 256 neurons per layer, which is less if compared with the 4096 neurons used by AlexNet. The use of smaller FC layers is based on the intuition that a less capable classifier stage enforces learning more distinctive convolutional features. Furthermore, we observe that using a full precision FC stage improves the overall VPR performance and makes the training faster. Indeed, a BNN requires a longer training time because of the noise-induced by binary weights and activations in the loss function [4]. Thus, having fewer binary weights in the network decreases the noise and the learning time. It is relevant mentioning that FC stage tuning is applicable only when VPR is carried out with convolution features as the tuned FC stage is removed from the model (Figure 4.B).

## IV. EXPERIMENTAL SETUP

This section provides details about the experimental setup (including evaluation criteria, training and test datasets) used for assessing the VPR performance of the binary neural networks presented later in Section IV-D.

### A. Evaluation Criteria

In our experiments, VPR is cast as a loop closure detection task [6]. Reference images showing already visited locations are searched to find the best match with the robot camera's current view, namely the query image. VPR is considered successful when a query image is paired with one of the correct reference images. The image descriptors used to match images are obtained by L2-normalization of a network's layer output:

$$D = \frac{\hat{X}_l}{\|\hat{X}_l\|_2}, \quad (5)$$

where  $\hat{X}_l$  is the output of the  $l^{th}$  layer.

Descriptors are compared using Euclidean distance; the shorter the distance, the higher the similarity between two images.

$$d = \|D_1 - D_2\|_2, \quad (6)$$

where  $D_1$  and  $D_2$  are the image descriptors to be compared. The reference image with the shortest distance from the query is regarded as the current location.

Following the approach proposed in [16], VPR is evaluated on a whole dataset with  $S_{P100}$  index. It represents the ratio of places that are correctly recognized against the ground truth.

VPR performance is also evaluated in relation to memory requirements. We define memory efficiency as the ratio of  $S_{P100}$  to the model size:

$$\eta_m = \frac{S_{P100}}{M_{size}} \quad (7)$$



$\eta_m$  indicates the memory cost per point of  $S_{P100}$ . The smaller  $\eta_m$ , the higher the efficiency of a network in using memory.

### B. Training Data

The data used to train all the models is Places365 [49], [2]. It is a place-themed dataset consisting of 1,803,460 images divided into 365 categories with between 3068 and 5000 images in each category. The validation set includes 100 images per location class.

### C. Test Data

On long term runs, a robot visits a place at different times or from different directions. These factors yield changes in the appearance of places captured by the robot’s camera. In order to provide comprehensive results, test data includes five datasets, each containing environmental and/or viewpoint changes, as shown in Table I. All datasets have two subsets that correspond to different traverses of the environment (Figure 5). One is the reference dataset representing the previous knowledge of the environment while the other is the query dataset that represents the current traverse. The datasets include a different number of query images. To compute fair average performance indicators (e.g. Table VI), we randomly sampled 200 query images from each of them for a total of 1000 images.

The datasets are detailed below and summarized in Table I.

1) *GardenPoints Walking* [43]: This dataset includes three traverses of the Queensland University of Technology (QUT). The experiments employed Right-Day and Right-Night to test VPR under illumination changes and mild lateral shifts. Ground truth is built by frame correspondences with a tolerance of  $\pm 2$  frames [33].

2) *Berlin Kudamm* [9]: It consists of two traverses captured in an urban environment with moderate to strong lateral shifts. Dynamic objects, such as cars and pedestrians, contribute to modify the environment’s appearance. GPS coordinates have been used to build place-level correspondences with a tolerance of 50 meters.

3) *Nordland* [42]: It is built from synchronized footage captured along a rail track in Norway in four seasons. The experiment employed Summer and Winter journeys as reference and query datasets, respectively. The ground truth is built with a tolerance of  $\pm 5$  frames [33].

TABLE I  
TEST DATASETS AND GROUND TRUTH TOLERANCE.

Dataset	Viewpoint	Conditional	Reference Images	Ground Truth
GardenPoints	Lateral	Day-Night	200	$\pm 2$ frames
Berlin Kudamm	Lateral	Dynamic Objects	201	50 m
Nordland	None	Summer Winter	309	$\pm 5$ frames
Lagout	6-DOF	None	332	by authors
Old City	6-DOF	None	6708	by authors



Fig. 5. A corresponding image pair from each test datasets.

4) *Lagout* [35]: It is a synthetic dataset consisting of several flybys at different heights of a medieval building. The traverses at  $0^\circ$  and  $15^\circ$  are used as reference and query datasets respectively to test VPR under moderate viewpoint changes. The ground truth data is available from authors [3].

5) *Old City* [35]: It is an urban dataset with two traverses showing the same location from different perspectives to generate the viewpoint variation experienced by a 6-DOF (degrees-of-freedom) aerial robot. The ground truth data is available from authors [3].

### D. Binary Network and Comparison Baseline

The networks used for the experiments are based on the AlexNet archetype [29], which is one of the most used network type for VPR [9], [45], [5], [26]. AlexNet-type networks’ structure consists of several convolution blocks (CB) alternated with pool layers and followed by a fully connected (FC) stage with one or more hidden layers.

The baseline CNN is very similar to a standard AlexNet [29] except for the use of BatchNorm and pool layers with a  $2 \times 2$  non-overlapping kernel for higher accuracy [29]. The baseline has five convolution blocks followed by a fully connected stage with two hidden layers including 4096 neurons each. The detailed structure is shown in Table II using the following notation.  $C(k, s, h)$  indicates a convolution block with kernel size  $k$ , stride  $s$  and  $h$  channels (filters). A similar notation is used for max pool:  $P(k, s)$ . Fully connected layers are indicated with  $FC(n)$ , where  $n$  is number of neurons. The model sizes reported in Table II are cumulative and measure the model sizes at every network depth. For example, if the baseline is cut to use  $fc6$  features, the corresponding size of the model is 158.32 MiB.

BinaryNet is obtained by binarization of the baseline as detailed in Section III-A. The bottom part of Table II shows the number of binarizable parameters. The remaining 32-bit parameters are due to BatchNorm as described in Section III-A3. However, their contribution to the binary model size is negligible. BinaryNet sizes vary from the 3.12% of Baseline at *conv1*, which is not preceded by a BatchNorm layer, to 3.18% at *pool5*.

### E. FloppyNet

FloppyNet consists of three binary convolution blocks and three pool layers as shown in Figure 6. Binarization, jointly with depth reduction applied to Baseline, resulted in a compact model of 154 Kib. The layers removed in depth reduction step are *conv3* and *conv4*. The output layer of FloppyNet is denoted as *pool5* by convention. We kept the same name as in the

TABLE II

BASELINE STRUCTURE AND MODEL SIZE BEFORE AND AFTER BINARIZATION. SIZE RATIO INDICATES THE RATIO BETWEEN THE BINARIZED AND FULL PRECISION MODEL SIZES.

Baseline Structure										
	conv1	pool1	conv2	pool2	conv3	conv4	conv5	pool5	fc6	fc7
Layer Setup	C(11,4,96)	P(2,2)	C(5,1,256)	P(2,2)	C(3,1,384)	C(3,1,384)	C(3,1,256)	P(2,2)	FC(4096)	FC(4096)
Features Size	290400	290400	186624	43264	64896	64896	43264	9216	4096	4096
Total Parameters (M)	0.03	0.04	0.65	0.65	1.54	2.86	3.75	3.75	41.5	58.29
Model Size (MiB)	0.13	0.13	2.48	2.48	5.86	10.92	14.3	14.3	158.32	222.37
Binarizable Params. (M)	0.03	0.03	0.65	0.65	1.53	2.86	3.75	3.75	41.49	58.27
Non-Binarizable Params.	0	0	192	192	704	1472	2240	2240	2752	10944
Binary Model Size (KiB)	4.25	4.25	80	80	190	355	466	466	5076	7156
Model Size Ratio (%)	3.12	3.1	3.15	3.15	3.17	3.17	3.18	3.18	3.13	3.14

TABLE III

FLOPPYNET FEATURE EXTRACTOR STRUCTURE AND MODEL SIZES.

FloppyNet Structure						
	conv1	pool1	conv2	pool2	conv5	pool5
Layer Setup	C(11,4,96)	P(2,2)	C(5,1,256)	P(2,2)	C(3,1,256)	P(2,2)
1-bit parameters	0.03	0.03	0.65	0.65	1.24	1.24
32-bits parameters	0	0	192	192	704	704
Model Size (KiB)	4.25	4.25	80	80	154	154
Model Size Ratio - BinaryNet (%)	100	100	100	100	33.05	33.05
Model Size Ratio - Baseline (%)	3.12	3.1	3.15	3.15	1.05	<b>1.05</b>

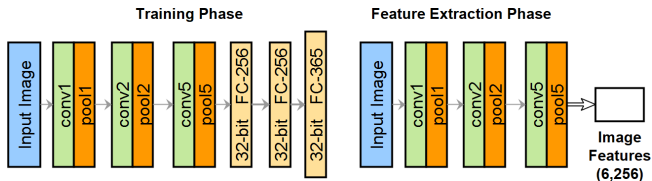


Fig. 6. FloppyNet layer structure. The output features used for VPR are from *pool5* layer.

baseline since they have the same structure and both provide feature vectors with the same shape and element number:  $6 \times 6 \times 256 = 9216$  elements.

The primary motivation of FloppyNet is to further reduce the model size from BinaryNet. FloppyNet uses the 33% of the memory of BinaryNet at *pool5* and 1% of the memory required by the baseline (Table III). Binarization and depth reduction cause a performance loss that is mostly compensated by tuning the FC stage properly for the training. Our best model is obtained with 256 full precision neurons in both *fc6* and *fc7*. This training approach’s effectiveness is demonstrated in Section V-B where FloppyNet is compared against ShallowNet, a network trained without tuning the FC stage.

## V. RESULTS AND DISCUSSION

The experimental results are organized in several paragraphs as follows. The first part provides a detailed analysis of features from every layer in both the baseline and BinaryNet. The results obtained drive the design of FloppyNet towards the use of *pool5* as an output layer. In the second part, the performance of FloppyNet and its memory efficiency are compared against deeper and full precision networks. This section concludes with a discussion on how binarization, depth

reduction, and FC stage tuning impact VPR performance when applied separately and in relevant combinations.

### A. BNN Layer Analysis

The first question to answer when a convolutional network is employed as a feature extractor is: Which layer’s output is the most suitable to build a distinctive image descriptor? CNNs can learn features at different levels of abstraction. Convolutional features retain some spatial information. However, as the depth increases, pool layers induce the loss of such spatial information in favor of translation invariance. In fully connected layers, the activation of a neuron depends on every neuron in the previous level. Hence, the spatial information vanishes while improving the invariance to viewpoint changes and translation in particular [22]. The second question we need to answer is how binarization impacts layers’ features and VPR matching performance.

The answers to these questions are given in Table IV and Table V, which show  $S_{P100}$  for every layer of the baseline and BinaryNet, respectively.

In the Baseline, deeper convolutions and fully connected layers handle viewpoint changes better than others. *Fc6* and *fc7* obtain the highest performance under extreme viewpoint changes that characterize Old City. *Pool5* is the best on GardenPoints, which includes mild viewpoint shifts other than day-light variations. On the other hand, shallower layers deal better with appearance changes. Nordland includes only seasonal variations, and the best is *conv4* with  $S_{P100} = 95\%$ . These results partially confirm findings of a previous study on a standard AlexNet [22], which indicates *conv3* as the best layer to deal with appearance changes while *pool5* and, in

TABLE IV  
 $S_{P100}$  FOR EVERY LAYER IN BASELINE.

Baseline Image Features										
	conv1	pool1	conv2	pool2	conv3	conv4	conv5	pool5	fc6	fc7
GardenPoints	14.5	29	56.5	62.5	67	79.5	66	84	73	56.5
Berlin Kudamm	7	5	6	6	6	5.5	7.5	8	9.5	14
Nordland	69	75.5	86.5	91	91	95	54	85	40	29
Lagout	71.5	88	94	96	98.5	99.5	98	100	100	100
Old-City	7	11	7	9	11	18	13	33	39	37
Average	33.8	41.7	50	52.9	54.7	59.5	47.7	<b>62</b>	52.3	47.3

TABLE V  
 $S_{P100}$  FOR EVERY LAYER IN BINARYNET.

BinaryNet Image Features										
	conv1	pool1	conv2	pool2	conv3	conv4	conv5	pool5	fc6	fc7
GardenPoints	3	11.5	43	51.5	75.5	74.5	76	79.5	66.5	39.5
Berlin Kudamm	6	7	8.5	9.5	8	8.5	7.5	8	8.5	8
Nordland	53	60	71.5	71	77.5	77	72	71.5	38.5	14
Lagout	53	71.5	83	90.5	90.5	99	100	100	100	100
Old-City	9	10.5	11.5	15	16	15	20.5	23	49	44.5
Average	24.8	32.1	43.5	47.5	53.5	54.9	55.2	<b>56.4</b>	52.5	41.2

some cases, *fc6* as the best choice to deal with viewpoint changes.

Binarization negatively affects VPR performance, but the characteristics of the layers are more or less unchanged. As shown in Table V, *pool5* achieves the highest performance on the same dataset as for the baseline. Similarly, fully connected layers outperform the others on Old city and Berlin Kudamm.

Overall, *pool5* is the layer that guarantees the highest average performance across the five datasets. The average  $S_{P100}$  is 62% for Baseline and 56.4% for its binary counterpart. The gap is moderate (5.6%), especially considering that BinaryNet at *pool5* requires only 3.18% of memory used by the baseline (Table II). The average  $S_{P100}$  is computed across all the datasets as they formed a single environment including five with 200 query images each. For a robot navigating such a working space, *pool5* features guarantee the most reliable and consistent VPR performance. Accordingly, we designed FloppyNet with the same shape progression of the features maps as in BinaryNet to have the output layer with similar characteristics as *pool5*. As detailed in Section IV-E, this is obtained by removing two inner convolution blocks: *conv3* and *conv4*.

### B. Comparative Results

FloppyNet is compared against several other networks. These include HybridNet, VGG-16, Baseline, BinaryNet and, ShallowNet. The latter is the version of FloppyNet trained with regular fully connected layers (4096 neurons). HybridNet [8] is a version of AlexNet with an additional convolution block trained on ImageNet and tuned on SPED dataset [8]. The results for HybridNet are obtained with *pool6* features. VGG-16 [41] is a very deep network if compared with FloppyNet since it includes 13 convolutional blocks. It is relevant to include VGG-16 in the comparison because several multi-staged VPR methods widely use it as a feature extractor.

Some examples are R-MAC [45], Cross-Region-Bow [9] and NetVLAD [5]. VGG-16 model has been trained from scratch using Places365, and the features used for the tests are from the very last pool layer.

Figure 7 shows  $S_{P100}$  for the considered networks. VGG-16 is the best on every dataset except on Old City, where HybridNet outperforms it by a close gap. FloppyNet obtains lower but comparable performance with Baseline. The most substantial gap is on Garden Point, where the Baseline scores  $S_{P100} = 84$  against 75.5 of FloppyNet.

FloppyNet outperforms ShallowNet on Nordland and Old City. Only on Garden Point, ShallowNet is better than FloppyNet but by a very narrow margin.

### C. Memory Efficiency

Table VI shows the memory efficiency for all the compared networks.  $S_{P100}$  is the average score on the five datasets as described in Section V-A. Binary networks have extremely low  $\eta_m$  values compared to any full precision network. FloppyNet requires 2.65 KiB per  $S_{P100}$  point, while the more efficient full precision model is the baseline with  $\eta_m = 236.3$  Kib. ShallowNet has the same size as FloppyNet but lower  $S_{P100}$ , hence slightly worse efficiency: 2.77 Kib.

### D. Projected Computation Speed-up

The total number of MACs in a network can be easily determined from layers' hyperparameters [44]. The Baseline has five convolutions and computes 711 MACs to obtain an image representation at *pool5*. FloppyNet has two layers less than Baseline for a total of 653M MACs, of which 547.6M are binary (83.9%). The rest 105.5M are from BatchNorm and the input layer. Considering that a binary MAC is 5.3 faster

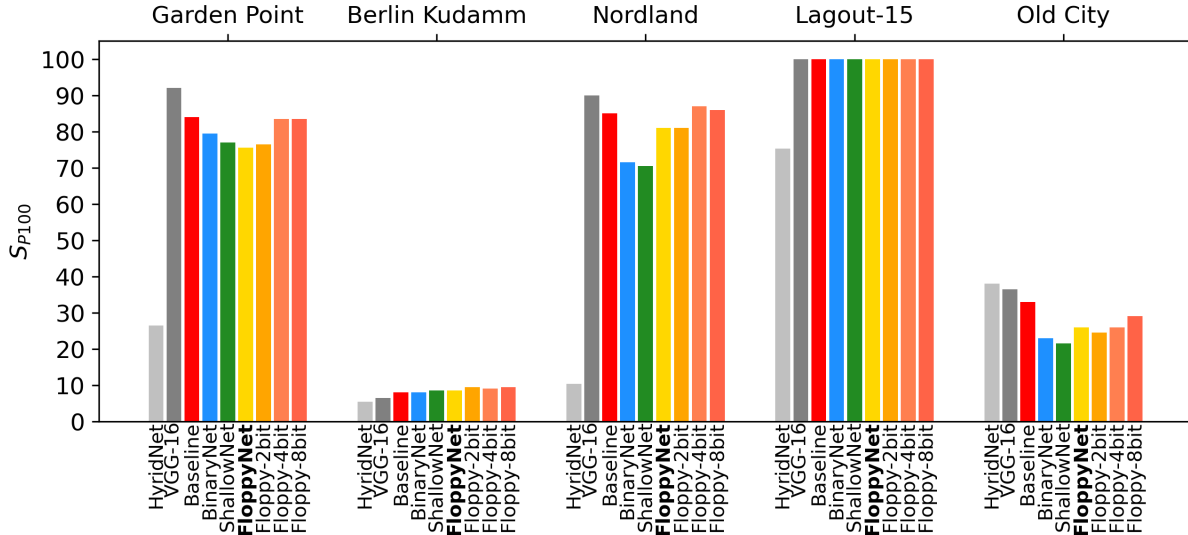


Fig. 7. VPR comparison on five test datasets.

(Section III-A2) and fewer parameters, FloppyNet can be up to 3.4 times faster.

$$\text{Speed-up} = \frac{711}{547/5.3 + 105.5} = 3.4 \quad (8)$$

### E. Higher Precision Models

The comparative analysis presented in Figure 7 includes 2-bit, 4-bit and 8-bit versions of FloppyNet. While Floppy-2bit exhibits similar performance as FloppyNet, the 4-bit model performs better. In particular, Floppy-4bit outperforms FloppyNet in every test scenario and has comparable average  $S_{P100}$  to the baseline: 61.02 versus 62 (Table VI). Although Floppy-4bit requires about six times the memory of FloppyNet,  $\eta_m$  is 9.25 KiB, which is far better than any considered full precision network. Therefore, Floppy-4bit might be an excellent alternative to FloppyNet when a robot has some extra memory available. Finally, increasing the quantization to 8 bits does not provide any tangible benefits (as  $\eta_m$  increases from 9.96 KiB for the 4-bit model to 19.74 KiB for Floppy-8bit).

TABLE VI  
MEMORY COST (KiB) PER AVERAGE  $S_{P100}$  POINT.

	Precision	$S_{P100}$	Size (KiB)	$\eta_m$
HybridNet	Full	33.57	16957	505.12
Baseline	Full	62	14648	236.3
VGG-16	Full	66.13	57487	869.3
BinaryNet	1-bit	56.4	466	8.26
ShallowNet	1-bit	55.5	154	2.77
<b>FloppyNet</b>	<b>1-bit</b>	<b>58.2</b>	<b>154</b>	<b>2.65</b>
FloppyNet-2	2-bit	58.22	306	5.26
FloppyNet-4	4-bit	61.02	608	9.96
FloppyNet-8	8-bit	61.52	1213	19.72

### F. Binarization, Depth Reduction and FC-256

Figure 8 shows  $S_{P100}$  relative to Baseline resulting from using binarization (Bin), depth reduction (Depth), and FC stage tuning (FC256) separately and their relevant combinations. The features used to obtain the results are from *pool5* layer.

Depth reduction (Depth) yields a full precision network with better performance on Nordland. Depth reduction makes the output layer of a model retain more spatial information compared to the baseline. Hence, the better performance on the seasonal changes of the Nordland dataset. Depth reduction positively affects the performance on Berlin Kudamm as well. This dataset includes two significant sources of variations: viewpoint change and dynamic objects. However, these results might not be conclusive because the VPR performance is generally low on Berlin Kudamm (Figure 7). Small variations of  $S_{P100}$ , such as those due to the training's stochastic nature, can cause relatively large variations. Training a full precision model with 256 neurons in the FC stage (FC256) helps VPR significantly to tackle extreme 6-DOF viewpoint variations. FC256 model achieves 25% higher  $S_{P100}$  on Old City than the original model trained with 4096 neurons in the FC stage. In classifiers, the FC stage is usually sized as large as possible to maximize accuracy while avoiding overfitting. Conversely, the empirical evidence shows that VPR benefits from a smaller FC stage. These results suggest that the FC stage has different roles in classification and VPR tasks.

Depth reduction does not help  $S_{p100}$  scores of the binarized models. The values of  $S_{p100}$  for binary (bin) and shallow binary networks (bin+dep) are very close to each other on every test dataset (and Nordland in particular), which is rather unexpected considering the full precision case (Depth). The red bars in Figure 8 represent FloppyNet, which implements all the steps of the proposed approach. The addition of FC stage tuning counters the  $S_{p100}$  loss due to binarization and depth reduction in every tested scenario (except Garden Point)



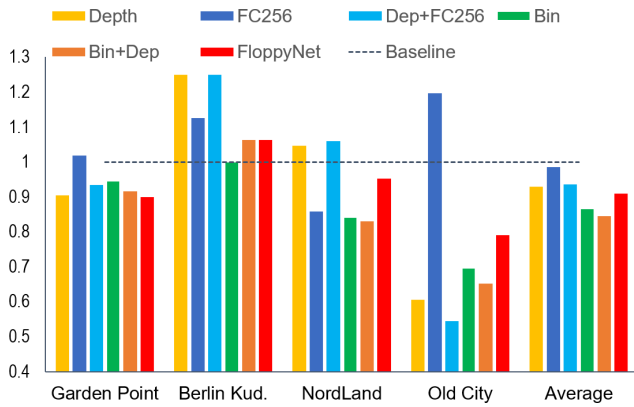


Fig. 8.  $SP_{100}$  relative to Baseline (dotted line) of several combinations of the three techniques used by FloppyNet: depth reduction, binarization and training with a weak fully connected stage. The features used for VPR are from *pool5* layer. Lagout is not included because  $SP_{100} = 100$  for every model.

proving the effectiveness of the proposed training approach.

## VI. CONCLUSION

This paper proposes FloppyNet, a compact binary network to solve the VPR problem. FloppyNet achieves comparable VPR performance as deeper and full precision networks in changing environments with drastically lower memory requirements. A network with such a small memory footprint opens up several opportunities for embedded systems. FloppyNet may be employed on very cheap hardware to enable VPR or replace existing networks to save resources to implement additional functionalities for autonomous robotic navigation. For example, several state-of-the-art image descriptors, such as Cross-Region-Bow and NetVLAD, use a VGG-M model to extract image features that are subsequently post-processed to compute a robust image representation. If FloppyNet is used instead, the memory requirements of both Cross-Region-Bow and NetVLAD would decrease dramatically. This suggests that a natural extension of this work would be to investigate feature pooling and post-processing techniques applied to BNNs.

## REFERENCES

- [1] CUDA Toolkit Documentation. <https://docs.nvidia.com/cuda/cuda-c-programming-guide/index.html#arithmetic-instructions>. Accessed: 2020-07-26.
- [2] Places365 DevKit. [https://github.com/zhoubolei/places\\_devkit](https://github.com/zhoubolei/places_devkit). Accessed: 2020-07-26.
- [3] V4RL Wide-baseline Place Recognition Dataset. [https://github.com/VIS4ROB-lab/place\\_recognition\\_dataset\\_ral2019](https://github.com/VIS4ROB-lab/place_recognition_dataset_ral2019). Accessed: 2019-04-04.
- [4] M. Alizadeh, J. Fernández-Marqués, N. D. Lane, and Y. Gal. A systematic study of binary neural networks' optimisation. In *International Conference on Learning Representations*, 2019.
- [5] R. Arandjelovic, P. Gronat, A. Torii, T. Pajdla, and J. Sivic. Netvlad: CNN architecture for weakly supervised place recognition. In *Proceedings of the IEEE Conference on Computer Vision and Pattern Recognition*, pages 5297–5307, 2016.
- [6] D. Bai, C. Wang, B. Zhang, X. Yi, and X. Yang. Sequence searching with cnn features for robust and fast visual place recognition. *Computers & Graphics*, 70:270–280, 2018.
- [7] Y. Bengio, N. Léonard, and A. Courville. Estimating or propagating gradients through stochastic neurons for conditional computation. *arXiv preprint arXiv:1308.3432*, 2013.

- [8] Z. Chen, A. Jacobson, N. Sünderhauf, B. Upcroft, L. Liu, C. Shen, I. Reid, and M. Milford. Deep learning features at scale for visual place recognition. In *2017 IEEE International Conference on Robotics and Automation (ICRA)*, pages 3223–3230. IEEE, 2017.
- [9] Z. Chen, F. Maffra, I. Sa, and M. Chli. Only look once, mining distinctive landmarks from convnet for visual place recognition. In *2017 IEEE/RSJ International Conference on Intelligent Robots and Systems (IROS)*, pages 9–16. IEEE, 2017.
- [10] F. Chollet et al. Keras. <https://keras.io>, 2015.
- [11] M. Courbariaux, Y. Bengio, and J.-P. David. Training deep neural networks with low precision multiplications. *arXiv preprint arXiv:1412.7024*, 2014.
- [12] M. Courbariaux, I. Hubara, D. Soudry, R. El-Yaniv, and Y. Bengio. Binarized neural networks: Training deep neural networks with weights and activations constrained to +1 or -1. *arXiv preprint arXiv:1602.02830*, 2016.
- [13] N. Dalal and B. Triggs. Histograms of oriented gradients for human detection. 2005.
- [14] S. K. Esser, J. L. McKinstry, D. Bablani, R. Appuswamy, and D. S. Modha. Learned step size quantization. *arXiv preprint arXiv:1902.08153*, 2019.
- [15] B. Ferrarini, M. Waheed, S. Waheed, S. Ehsan, M. Milford, and K. D. McDonald-Maier. Visual place recognition for aerial robotics: Exploring accuracy-computation trade-off for local image descriptors. In *2019 NASA/ESA Conference on Adaptive Hardware and Systems (AHS)*, pages 103–108. IEEE, 2019.
- [16] B. Ferrarini, M. Waheed, S. Waheed, S. Ehsan, M. J. Milford, and K. D. McDonald-Maier. Exploring performance bounds of visual place recognition using extended precision. *IEEE Robotics and Automation Letters*, 5(2):1688–1695, April 2020.
- [17] W. T. Freeman and M. Roth. Orientation histograms for hand gesture recognition. In *International workshop on automatic face and gesture recognition*, volume 12, pages 296–301, 1995.
- [18] L. Geiger and P. Team. Larq: An open-source library for training binarized neural networks. *Journal of Open Source Software*, 5(45):1746, Jan. 2020.
- [19] S. Han, J. Pool, J. Tran, and W. J. Dally. Learning both weights and connections for efficient neural networks. In *Proceedings of the 28th International Conference on Neural Information Processing Systems—Volume 1*, pages 1135–1143, 2015.
- [20] B. Hassibi and D. G. Stork. Second order derivatives for network pruning: optimal brain surgeon. In *Proceedings of the 5th International Conference on Neural Information Processing Systems*, pages 164–171, 1992.
- [21] Y. Hou, H. Zhang, and S. Zhou. Convolutional neural network-based image representation for visual loop closure detection. In *2015 IEEE International Conference on Information and Automation*, pages 2238–2245, 2015.
- [22] Y. Hou, H. Zhang, and S. Zhou. Convolutional neural network-based image representation for visual loop closure detection. In *2015 IEEE international conference on information and automation*, pages 2238–2245. IEEE, 2015.
- [23] I. Hubara, M. Courbariaux, D. Soudry, R. El-Yaniv, and Y. Bengio. Quantized neural networks: Training neural networks with low precision weights and activations. *The Journal of Machine Learning Research*, 18(1):6869–6898, 2017.
- [24] S. Ioffe and C. Szegedy. Batch normalization: Accelerating deep network training by reducing internal covariate shift. In *International Conference on Machine Learning*, pages 448–456, 2015.
- [25] H. Jégou, M. Douze, C. Schmid, and P. Pérez. Aggregating local descriptors into a compact image representation. In *CVPR 2010-23rd IEEE Conference on Computer Vision & Pattern Recognition*, pages 3304–3311. IEEE Computer Society, 2010.
- [26] A. Khaliq, S. Ehsan, Z. Chen, M. Milford, and K. McDonald-Maier. A holistic visual place recognition approach using lightweight cnns for significant viewpoint and appearance changes. *IEEE Transactions on Robotics*, pages 1–9, 2019.
- [27] A. Khaliq, S. Ehsan, M. Milford, and K. McDonald-Maier. Camal: Context-aware multi-scale attention framework for lightweight visual place recognition. *arXiv preprint arXiv:1909.08153*, 2019.
- [28] A. Khan, A. Sohail, U. Zahoora, and A. S. Qureshi. A survey of the recent architectures of deep convolutional neural networks. *Artificial Intelligence Review*, pages 1–62, 2020.
- [29] A. Krizhevsky, I. Sutskever, and G. E. Hinton. Imagenet classification with deep Convolutional Neural Networks. In *Advances in neural information processing systems*, pages 1097–1105, 2012.

- [30] Y. LeCun, J. S. Denker, and S. A. Solla. Optimal brain damage. In *Advances in neural information processing systems*, pages 598–605, 1990.
- [31] F. Li, B. Zhang, and B. Liu. Ternary weight networks. *arXiv preprint arXiv:1605.04711*, 2016.
- [32] D. G. Lowe. Distinctive image features from scale-invariant keypoints. *International journal of computer vision*, 60(2):91–110, 2004.
- [33] S. Lowry and M. J. Milford. Supervised and unsupervised linear learning techniques for visual place recognition in changing environments. *IEEE Transactions on Robotics*, 32(3):600–613, 2016.
- [34] F. Maffra, Z. Chen, and M. Chli. Viewpoint-tolerant place recognition combining 2d and 3d information for uav navigation. In *2018 IEEE International Conference on Robotics and Automation (ICRA)*, pages 2542–2549. IEEE, 2018.
- [35] F. Maffra, L. Teixeira, Z. Chen, and M. Chli. Real-time wide-baseline place recognition using depth completion. *IEEE Robotics and Automation Letters*, 2019.
- [36] M. J. Milford and G. F. Wyeth. Seqslam: Visual route-based navigation for sunny summer days and stormy winter nights. In *2012 IEEE International Conference on Robotics and Automation*, pages 1643–1649. IEEE, 2012.
- [37] M. Rastegari, V. Ordonez, J. Redmon, and A. Farhadi. Xnor-net: Imagenet classification using binary convolutional neural networks. In *European conference on computer vision*, pages 525–542. Springer, 2016.
- [38] D. Saad and E. Marom. Training feed forward nets with binary weights via a modified chir algorithm. *Complex Systems*, 4(5), 1990.
- [39] E. Sari, M. Belbahri, and V. P. Nia. How does batch normalization help binary training. *arXiv: Learning*, 2019.
- [40] T. Simons and D.-J. Lee. A review of binarized neural networks. *Electronics*, 8(6):661, 2019.
- [41] K. Simonyan and A. Zisserman. Very deep convolutional networks for large-scale image recognition. In *International Conference on Learning Representations*, 2015.
- [42] S. Skrede. Nordlandsbanen: minute by minute, season by season <https://nrkbeta.no/2013/01/15/nordlandsbanen-minute-by-minute-season-by-season/>.
- [43] N. Sünderhauf, S. Shirazi, F. Dayoub, B. Upcroft, and M. Milford. On the performance of convnet features for place recognition. In *2015 IEEE/RSJ International Conference on Intelligent Robots and Systems (IROS)*, pages 4297–4304, 2015.
- [44] M. Taghavi and M. Shoaran. Hardware complexity analysis of deep neural networks and decision tree ensembles for real-time neural data classification. In *2019 9th International IEEE/EMBS Conference on Neural Engineering (NER)*, pages 407–410. IEEE, 2019.
- [45] G. Tolias, R. Sivic, and H. Jégou. Particular Object Retrieval With Integral Max-Pooling of CNN Activations. In *ICLR 2016*, International Conference on Learning Representations, pages 1–12, San Juan, Puerto Rico, May 2016.
- [46] M. Zaffar, S. Ehsan, M. Milford, D. Flynn, and K. McDonald-Maier. Vpr-bench: An open-source visual place recognition evaluation framework with quantifiable viewpoint and appearance change. *arXiv preprint arXiv:2005.08135*, 2020.
- [47] M. Zaffar, A. Khaliq, S. Ehsan, M. Milford, K. Alexis, and K. McDonald-Maier. Are state-of-the-art visual place recognition techniques any good for aerial robotics? *arXiv preprint arXiv:1904.07967*, 2019.
- [48] M. Zaffar, A. Khaliq, S. Ehsan, M. Milford, and K. McDonald-Maier. Levelling the playing field: A comprehensive comparison of visual place recognition approaches under changing conditions. *arXiv preprint arXiv:1903.09107*, 2019.
- [49] B. Zhou, A. Lapedriza, A. Khosla, A. Oliva, and A. Torralba. Places: A 10 million image database for scene recognition. *IEEE transactions on pattern analysis and machine intelligence*, 40(6):1452–1464, 2017.
- [50] S. Zhou, Y. Wu, Z. Ni, X. Zhou, H. Wen, and Y. Zou. Dorefa-net: Training low bitwidth convolutional neural networks with low bitwidth gradients. *arXiv preprint arXiv:1606.06160*, 2016.
- [51] C. Zhu, S. Han, H. Mao, and W. J. Dally. Trained ternary quantization. *arXiv preprint arXiv:1612.01064*, 2016.